IMU-Based Indoor Localization for Construction Applications

Magdy Ibrahim[a] and Osama Moselhi[b]

[a]Department of Building, Civil & Environmental Engineering, Concordia University, Canada
[b]Department of Building, Civil & Environmental Engineering, Concordia University, Canada
E-mail: Magdy.omar@yahoo.com, moselhi@encs.concordia.ca

ABSTRACT

Localization and tracking of resources on construction jobsites is an emerging area where the location of materials, labour, and equipment is used to estimate productivity, measure project's progress and/or enhance jobsite safety. GPS has been widely used for outdoor tracking of construction operations. However, GPS is not suitable for indoor applications due to the lack of signal coverage; particularly inside tunnels or buildings. Several indoor localization research had been attempted, however such developments rely heavily on extensive external communication network infrastructures. These developments also are susceptible to electromagnetic interference in noisy construction jobsites. This paper presents indoor localization system using a microcontroller equipped with an inertial measurement unit (IMU). The IMU contains a cluster of sensors: accelerometer, gyroscope and magnetometer. The microcontroller uses a direct cosine matrix algorithm to fuse sensors data and calculate non-gravitational acceleration using nine-degrees-of-freedom motion equations. Current position is calculated based on measured acceleration and heading, while accounting for growing error in speed estimation utilizing jerk integration algorithm. Experimental results are presented to illustrate the relative effectiveness of the developed system, which is able to operate independently of any external aids and visibility conditions.

Keywords –
Indoor Localization; IMU; Jerk Integration

1 Introduction

The fact that indoor localization research is to date a very active research area indicates that there are still many challenges left to resolve. The challenges depend on the required accuracy and reliability dictated by the application. Recent advances in sensing technologies have enabled the deployment of a wide range of technologies for identification, location sensing, and tracking the movements of resources. Consequently many research works had been developed for resource and asset tracking, earthmoving operations, surveying, safety hazards predicting, and context aware construction [1-10].

Over the past few years, several researchers have experimented with indoor positioning technologies, which can be grouped in three major categories: (1) wave propagation; (2) image based; and (3) inertial navigation. Wave propagation technologies are based on the physical propagation properties of radio, ultrasonic or sound waves over distances [11-16]. Ultra wideband, infrared, WLAN and RFID are examples for radio frequency (RF) localization technology. However, several limitations for utilizing these technologies, had been reported by researchers. The infrared technology provides room-level accuracy and performs poorly in the presence of sunlight [16]. WLAN technology localization accuracy had been investigated by different researchers, and found to be varying from 4–9 m depending on localization algorithm utilized and number of WLAN access points [17-19]. Varying accuracies of RFID localization systems had been reported by researchers, from 5–9m depending on tags' configuration and the density of tag deployment [20-22]. Ultra wideband-based systems have a very high accuracy of approximately 20 cm [23], however the cost of commercially available ultra wideband localization systems is very high. Ultrasound technology is based on sound wave propagation. The reported accuracy of an ultrasound system is 9 cm [23], however, it requires line of sight for deployment of transmitters, and the cost is comparable to ultra wideband transmitters [16].

Image-based localization technology involves image matching and computer vision techniques. Computer vision techniques have been categorized as (1) global methods such as edge detection and feature recognition, and (2) local methods based on landmark detection using visual tags or image matching [24]. However, these methods yield coarse accuracy (room-level) and are

susceptible to occlusions and changes in the environment.

Inertial navigation localization technology utilizes an accelerometer and a gyroscope for sensing and detecting motion. The accelerometer measures acceleration in three dimensional spaces. The displacement is calculated by double integration of the acceleration. The gyroscope combined with the accelerometer is used to calculate the heading. This principle is called dead reckoning technique [25]. The dead reckoning is based on fusing the acceleration, and heading direction during a time step to determine how far and in what direction the user has moved from last known position. Unlike WLAN and RFID, motion sensing technology is independent from any infrastructure [26]. However, accelerometers are susceptible to acceleration caused by random movements, which might not necessarily be human motion, and magnetometers are susceptible to magnetic fields generated by electrical equipment and electronics [26]. Overall, motion sensing does not provide high location accuracies, but the accuracy can be improved by smart algorithms, which able to correct drift errors [27].

Several researchers attempt to use inertial navigation in construction, Joshua [28] applied accelerometers to classify workers' masonry activities in order to investigate workers' productivity. Taneja [29] investigated inertial measurement unit (IMU) sensors for location-tracking in a building site as compared to other sensors that used to establish local area networks (WLAN) and radio frequency identification (RFID).

Although significant research attempts has been done in developing several indoor localization systems using various technologies, the performance of these systems still expensive and not robust enough for usage in dense and noisy indoor environments such as construction jobsites. Further research work is needed to develop robust, cost effective and accurate indoor localization solutions for supporting rugged construction applications, such as automated progress reporting and jobsite safety.

This paper presents a newly developed extension to the inertial navigation technique for indoor localization system using a microcontroller equipped with an inertial measurement unit (IMU). This extension is intended to reduce accumulated errors in measured acceleration and heading utilizing a jerk integration algorithm.

2 Developed Method

The developed method encompassed hardware prototypes and software algorithms. The hardware development consists of a microcontroller equipped with an inertial measurement unit (IMU) and barometric pressure sensor as shown in Figure 1.

The IMU incorporates three sensors - an ITG-3200 (MEMS triple-axis gyro), ADXL345 (triple-axis accelerometer), and HMC5883L (triple-axis magnetometer), which gives 9 degrees of inertial measurement. The barometric pressure sensor provides the tenth degree of freedom for the system.

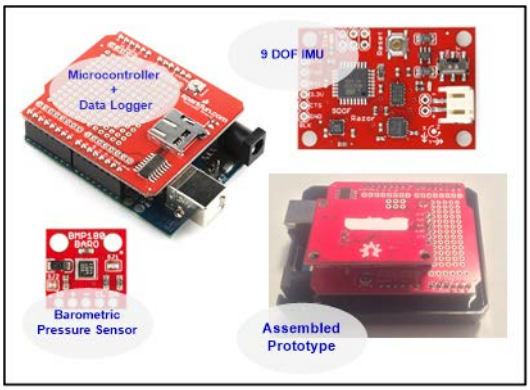

Figure 1. Developed Hardware Prototype

The outputs of all sensors are processed by an on-board ATmega328 processor and output over a serial interface. This hardware configuration provides 10 degrees of freedom to calculate the current position in three dimensional spaces as shown in figure 2.

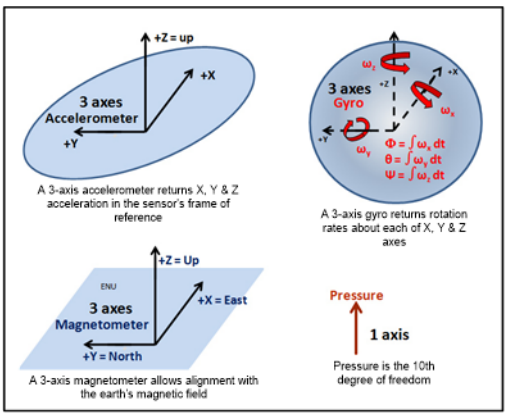

Figure 2. 10 Deg. of Freedom Measurement System

The software development consists of three modules, namely: inertial measurement module, altitude measurement module and localization module as shown in figure 3. The inertial measurement module processes and fuses inertial sensors using a Direction Cosine Matrix (DCM) algorithm. This algorithm accounts for gyro drift correction using accelerometer (gravity) vector and the magnetometer (compass) vector, and also compensates for tilt on X and Y magnetic components and provide correction for yaw angle magnetic heading. The altitude measurement module calculates the altitude based on the measured barometric pressure taking into account current weather condition (humidity, temperature… etc..).

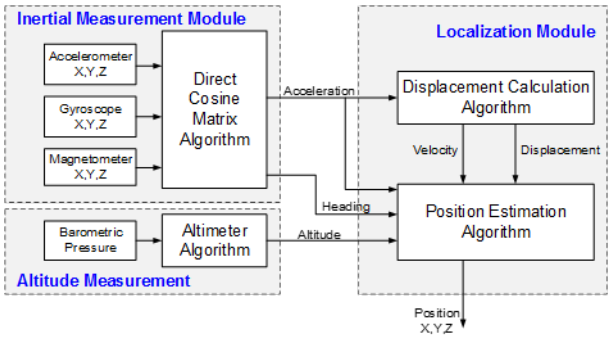

Figure 3. Developed Method

The localization module calculates current position based on acceleration, heading and barometric pressure data from the data acquisition module. The linear displacement is calculated using the displacement calculation algorithm by differentiation of the measured acceleration to calculate the jerk and then triple-integrates the jerk to calculate velocity and distance. The differentiation allows to correct DC margin errors in accelerometer readings and provides detection for detection of zero velocity intervals. The position estimation algorithm estimates current position based on calculated displacements, heading and altitude using Kalman filter. A detailed description of these algorithms is presented in the following sections with their mathematical background.

2.1 Displacement Calculation Algorithm

Traditionally the displacement is calculated by double integration of acceleration, however the global displacement error will grow by time due to drift associated with DC bias in the acceleration signal. To minimize these errors, a triple integration approach is presented in this research, where the acceleration is first differentiated to calculate the rate of change of acceleration (jerk). The jerk also allows for removal of gravity acceleration components.

Jerk can be defined as the changing rate of acceleration with respect to time [30], and its international unit is m/s3. According to Newton's second law of motion, jerk is viewed as the change of force magnitude for a unit mass in unit time. In recent years, jerk is applied in the tracking and positioning for Global Positioning System (GPS), the high-speed dynamic vehicle tracking, the automatic control of high-speed machines, and comfort evaluation for high speed trains and elevators [31–33]. It is obvious that the jerk and the integral of the displacement with respect to time also have determined an important significance.

The jerk value can be calculated by solving the time derivative of acceleration.

$$\text{Jerk} = \frac{\text{d(Acceleration)}}{\text{dt}} \qquad (1)$$

Then the jerk is triple integrated using numerical integration method to obtain the acceleration, velocity, and displacement. Some traditional integration methods such as the Newmark method and Wilson-θ method are commonly used in earthquake engineering for jerk integration, however these methods assume that the acceleration is constant or linear variation during the interval of time [34, 35], which will lead to the jerk in the interval, is assumed to be 0 or a constant, and this assumption is not in accordance with the real condition. In order to account for the variable acceleration and produce less errors than the normal integration, the trapeze integration method is used in this study.

$$Acceleration_t = \frac{(Jerk_{t-1} - Jerk_t)}{2} \times dt \qquad (2)$$

2.2 Floor Estimation

It is well known that atmospheric pressure decreases as altitude increases. Models for typical relationship between atmospheric pressure and altitude has been developed by many researchers as shown in Figure 4. According to these models atmospheric pressure drops by about 0.11hPa for every 1m increase in height.

With the measured pressure P and the pressure at sea level P_0 e.g. 1013.25hPa, the altitude in meters can be calculated with the international barometric formula:

$$Altitude = 44330 \times \left(1 - \left(\frac{P}{P_0}\right)^{\frac{1}{5.255}}\right) \qquad (3)$$

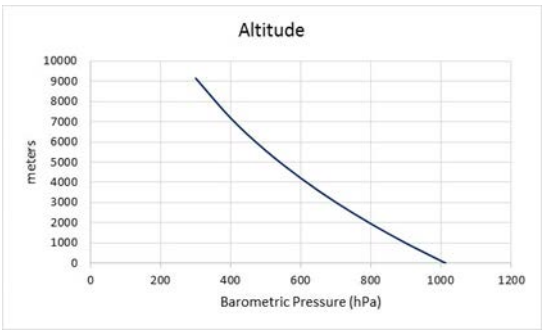

Figure 4. Altitude vs Atmospheric Pressure

The reference sea level pressure is obtained for weather stations which report online their air pressure in real time with the height of the station.

While the process of estimating the altitude from the barometric pressure sensor seems straight forward, there are other issue need to be taken into account. Barometric pressure sensors are normally calibrated for standard atmosphere conditions such as dry air with 15°C temperature and 1013.2hPa pressure. A correction factor must be considered for different weather conditions.

Also the latency of air pressure can cause a significant error in the sensor reading, however, in the case of indoor localization such factor can be neglected. As our testing indicated that there is about 0.42hPa change in the air pressure due to a change of one floor, which is significantly larger than the sensor measurement noise (0.02hPa for pressure sensor BMP180).

2.3 Position Estimation Algorithm

The position estimation algorithm is based utilizes Kalman filter, which was first introduced in 1960 to present a solution for discrete data linear filtering problem [36]. Since then, extensive research and application had been proposed, particularly in the areas of robotics and navigation. The key advantage of the Kalman filter is its simple computational algorithm, and adaptive recursive nature [37]. Kalman filter estimation process is based on a feedback loop control system. Which first estimates the process's state at a point in time and then obtains feedback of measurements. This feedback measurement is used to adjust the model parameters for next estimate. The model assumes that the state of a system at a time t evolved from the prior state at time t-1 according to the equation

$$X_t = A_t X_{t-1} + B_t u_{t-1} + w_t \quad (4)$$

where X_t is the process state vector at time t, A_t is the state transition matrix which is applied to the previous state X_{t-1}, u_t is the control input vector, B_t is the control-input model which is applied to the control vector u_t, and w_t is the process noise which is assumed to be drawn from a zero mean multivariate normal distribution with covariance Q_t.

At time t a measurement Z_t of the true state X_t is calculated according to

$$Z_t = H_t X_t + v_t \quad (5)$$

Where H_t is the measurement model for mapping true state space into measurement space and v_t is the measurement noise which is assumed to be zero mean Gaussian white noise with covariance R_t.

The Kalman filter recursive estimator model as shown in Figure 5 has two phases, the prediction phase, which estimates the priori process state at next observation time, and the correction phase, which incorporates a new measurement into the a priori estimate to obtain an improved a posterior estimate.

In the context of the positioning algorithm described in this paper, the state vector x is a vector containing the position, velocity and acceleration data

$$X = [x \quad y \quad z \quad v_x \quad v_y \quad v_z \quad a_x \quad a_y \quad a_z]^T \quad (6)$$

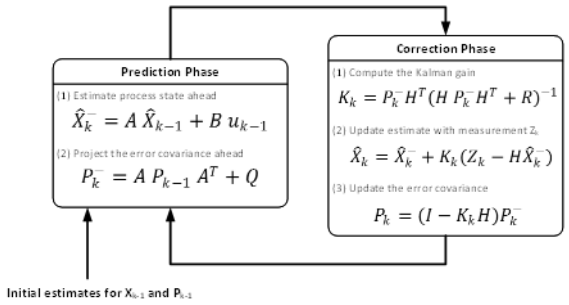

Figure 5. Kalman Filter Recursive Estimator Model

The process model relates the state at a previous time k-1 with the current state at time k is represented as follows:

$$\begin{bmatrix} x_k \\ y_k \\ z_k \\ v_{x_k} \\ v_{y_k} \\ v_{z_k} \\ a_{x_k} \\ a_{y_k} \\ a_{z_k} \end{bmatrix} = \begin{bmatrix} 1 & 0 & 0 & \Delta t & 0 & 0 & \frac{(\Delta t)^2}{2} & 0 & 0 \\ 0 & 1 & 0 & 0 & \Delta t & 0 & 0 & \frac{(\Delta t)^2}{2} & 0 \\ 0 & 0 & 1 & 0 & 0 & \Delta t & 0 & 0 & \frac{(\Delta t)^2}{2} \\ 0 & 0 & 0 & 1 & 0 & 0 & \Delta t & 0 & 0 \\ 0 & 0 & 0 & 0 & 1 & 0 & 0 & \Delta t & 0 \\ 0 & 0 & 0 & 0 & 0 & 1 & 0 & 0 & \Delta t \\ 0 & 0 & 0 & 0 & 0 & 0 & 1 & 0 & 0 \\ 0 & 0 & 0 & 0 & 0 & 0 & 0 & 1 & 0 \\ 0 & 0 & 0 & 0 & 0 & 0 & 0 & 0 & 1 \end{bmatrix} \begin{bmatrix} x_{k-1} \\ y_{k-1} \\ z_{k-1} \\ v_{x_{k-1}} \\ v_{y_{k-1}} \\ v_{z_{k-1}} \\ a_{x_{k-1}} \\ a_{y_{k-1}} \\ a_{z_{k-1}} \end{bmatrix} + W_{k-1} \quad (7)$$

The measurement model relates the current state to the measurement z with the matrix H is represented as follows:

$$\begin{bmatrix} x_k \\ y_k \\ z_k \end{bmatrix} = \begin{bmatrix} 1 & 0 & 0 & 0 & 0 & 0 & 0 & 0 & 0 \\ 0 & 1 & 0 & 0 & 0 & 0 & 0 & 0 & 0 \\ 0 & 0 & 1 & 0 & 0 & 0 & 0 & 0 & 0 \end{bmatrix} \begin{bmatrix} x_k \\ y_k \\ z_k \\ v_{x_k} \\ v_{y_k} \\ v_{z_k} \\ a_{x_k} \\ a_{y_k} \\ a_{z_k} \end{bmatrix} + V_k \quad (8)$$

The process is started by making an appropriate, optimal estimate of the state vector at an initial epoch. The coordinates are set at the values of (0, 0, 0) while the velocities, accelerations and jerk are set at zero. The variance of this initial optimal state vector can be assumed to be diagonal and appropriate values adopted.

Thereafter, at each epoch the following process is repeated:

1. Compute an estimate of the (predicted) state vector and its associated variance matrix from the optimal estimate of the state vector of the previous epoch.

2. From the observation equations by combining the predicted state vector and the IMU measurements of the velocity and acceleration.

3. Compute the least squares estimate of the state vector and associated variance matrix.

3 Experiments and Results

To examine the effectiveness of the developed method, several experiments have been performed for different localization scenarios. The developed prototype was mounted on using a belt clip on a human volunteer. The prototype processed the data and sent the personnel position wirelessly to a database application, which in turn stored the data with timestamps.

Experiments were performed in indoor laboratory environment at Concordia University, Construction Management Lab. Another set of experiments were performed in the corridors of Concordia University at Sir George Williams Campus. The experiment settings are summarized in Table 1. In these experiments, different paths were used for distance ranges from 5 meters to 260 meters. Different walking patterns were performed ranging from slow, fast to running, in order to check the consistency of the developed method.

Table 1 Experiments Description

Trial	Description	Duration	Distance
1	Slow Straight Line	7 s	5m
2	Fast Straight Line	24 s	25m
3	Running Straight Line	72 s	120m
4	Campus Walk	294 s	260m

In the campus walk experiment the path starts and ends at the same position. The path includes straight line walking and had several left and right turns. Also the path included climbing up and down several flights of stairs to check the accuracy of altitude measurement using the barometric pressure sensor signal as shown in Figure 6.

Figure 6. Campus Walk Path

Due to paper space limitations, only the result of the last experiment will be explained in details with a summary of all experiments results. Each experiment was repeated thirty times to appropriately assess the results. A total of 120 data sets collected with a total experimentation duration of 396 minutes.

The velocity in the x-axis before the jerk integration shows a drift in the calculated velocity, such drift is one of the reasons for the accumulated errors in the calculated position (Figure 7). The jerk integrator removed the constant bias in the velocity, and hence reduced the errors in position estimation.

Reducing errors in acceleration calculation through integration of the jerk, provides an effective way to remove gravity component in the measured acceleration and orientation errors, which cause huge drift error on long runs. An error in IMU orientation also could cause an incorrect projection of the acceleration signals onto global axes, which in turn causes wrong integration direction of the acceleration.

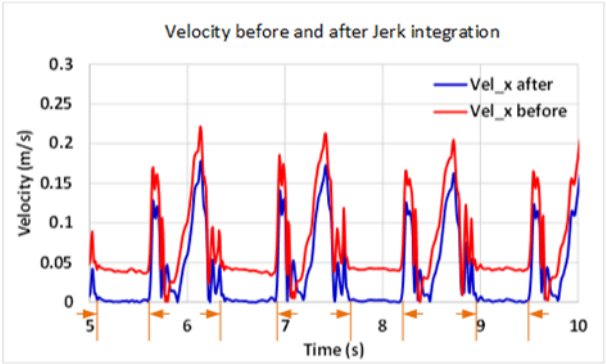

Figure 7. Velocity before and after Jerk Integration

Figure. 8 shows the 3D plot of the estimated walking path using the developed method. The results show that the estimated position follows the planned path very closely with an error of 3.67 m in 2D, between the start and end of the 260.79 m path. Hence the position estimation error is about 1.40% of the total travelled distance.

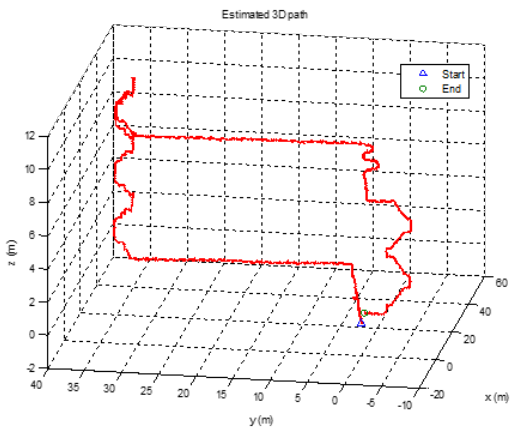

Figure 8. Estimated 3D Travel Path

The average drift error (as a percentage of the total travelled path length) for all experiments ranged from 0.32% for experiment trial 1 to 1.40% for experiment trial4 (an average of 30 runs). These errors are compared with previous research [29], where an off the shelf IMU localization system was utilized. Their experimental results showed a range of drift error from 1.92% to 6.2% for travel paths with length up to 250 m. It is clear that our developed method is able to estimate indoor position with higher accuracy.

4 Conclusions

This paper presented an extension to the inertial indoor localization method using IMU. The developed method encompassed hardware prototypes and software algorithms. The hardware development consists of a microcontroller equipped with an inertial measurement unit (IMU) and barometric pressure sensor. This hardware configuration provides 10 degrees of freedom to estimate the current position in three dimensional spaces.

This extension is designed to reduce accumulated drift errors in measured acceleration and heading utilizing a jerk integration algorithm. The results of several indoor testing experiment showed an average drift error ranging from 0.32% to 1.40% of the total travelled distances. The results were compared to previous research where the developed method showed significant improvement in the location drift errors.

References

[1] Caldas, C. H., Torrent, D. G., & Haas, C. T. (2006). Using global positioning system to improve materials-locating processes on industrial projects. Journal of Construction Engineering and Management, 132(7), 741-749. doi:10.1061/(ASCE)0733-9364(2006)132:7(741)

[2] Ergen, E., Akinci, B., & Sacks, R. (2007). Tracking and locating components in a precast storage yard utilizing radio frequency identification technology and GPS. Automation in Construction, 16(3), 354-367. doi:10.1016/j.autcon.2006.07.004.

[3] Goodrum, P. M., McLaren, M. A., & Durfee, A. (2006). The application of active radio frequency identification technology for tool tracking on construction job sites. Automation in Construction, 15(3), 292-302. doi:10.1016/j.autcon.2005.06.004

[4] Torrent, D. G., & Caldas, C. H. (2009). Methodology for automating the identification and localization of construction components on industrial projects. Journal of Computing in Civil Engineering, 23(1), 3-13. doi:10.1061/(ASCE)0887-3801(2009)23:1(3)

[5] Jang, W., & Skibniewski, M. J. (2008). A wireless network system for automated tracking of construction materials on project sites. Journal of Civil Engineering and Management, 14(1), 11-19. doi:10.3846/1392-3730.2008.14.11-19

[6] Khoury, H. M., & Kamat, V. R. (2009). High-precision identification of contextual information in location-aware engineering applications. Advanced Engineering Informatics, 23(4), 483-496. doi:10.1016/j.aei.2009.04.002

[7] Razavi, S. N., & Haas, C. T. (2010). Multisensor data fusion for on-site materials tracking in construction. Automation in Construction, 19(8), 1037-1046. doi:10.1016/j.autcon.2010.07.017

[8] Razavi, S. N., Young, D. A., Nasir, H., Haas, C., Caldas, C., Goodrum, P., & Murray, P. (2008). Field trial of automated material tracking in construction. Annual Conference of the Canadian Society for Civil Engineering 2008 - "Partnership for Innovation", June 10, 2008 - June 13, , 3 1503-1511.

[9] Song, J., Haas, C. T., Caldas, C., Ergen, E., & Akinci, B. (2006). Automating the task of tracking the delivery and receipt of fabricated pipe spools in industrial projects. Automation in Construction, 15(2), 166-177. doi:10.1016/j.autcon.2005.03.001

[10] Teizer, J., Venugopal, M., & Walia, A. (2008). Ultrawideband for automated real-time three-dimensional location sensing for workforce, equipment, and material positioning and tracking. Transportation Research Record, (2081), 56-64. doi:10.3141/2081-06

[11] Finkenzeller, K. (2003). RFID handbook: Fundamentals and applications in contactless smart cards and identification, Wiley, West Sussex, UK

[12] Guerrieri, J. R., Francis, M. H., Wilson, P. F., Kos, T., Miller, L. E., Bryner, N. P. Klein-Berndt, L. (2006). RFID-assisted indoor localization and communication for first responders. European Conference on Antennas and Propagation: EuCAP 2006, November 6, 2006 - November 10, , 626 SP

[13] Want, R., Hopper, A., Falcao, V., & Gibbons, J. (1992). Active badge location system. ACM Transactions on Information Systems, 10(1), 91-102. doi:10.1145/128756.128759

[14] Skibniewski, M. J., & Jang, W. (2007). Localization technique for automated tracking of construction materials utilizing combined RF and ultrasound sensor interfaces. 2007 ASCE International

Workshop on Computing in Civil Engineering, July 24, 2007 - July 27, 657-664. doi:10.1061/40937(261)78

[15] Kim, B., & Choi, J. (2007). Active beacon system with the fast processing architecture for indoor localization. 12th IEEE International Conference on Emerging Technologies and Factory Automation, ETFA 2007, September 25, 2007 - September 28, 892-895. doi:10.1109/EFTA.2007.4416875

[16] Hightower, J., & Borriello, G. (2001). Location systems for ubiquitous computing. Computer, 34(8), 57-66. doi:10.1109/2.940014

[17] Bahl, P., & Padmanabhan, V. N. (2000). RADAR: An in-building RF-based user location and tracking system. 19th Annual Joint Conference of the IEEE Computer and Communications Societies - IEEE INFOCOM2000: 'Reaching the Promised Land of Communications', March 26, 2000 - March 30, , 2 775-784.

[18] Elnahrawy, E., Li, X., & Martin, R. P. (2004). The limits of localization using signal strength: A comparative study. 2004 First Annual IEEE Communications Society Conference on Sensor and Ad Hoc Communications and Networks, 406-14.

[19] Deasy, T. P., & Scanlon, W. G. (2004). Stepwise algorithms for improving the accuracy of both deterministic and probabilistic methods in WLAN-based indoor user localisation. International Journal of Wireless Information Networks, 11(4), 207-16. doi:10.1007/s10776-004-1234-1

[20] Hightower, Jeffrey, Roy Want, and Gaetano Borriello. (2000). SpotON: An indoor 3D location sensing technology based on RF signal strength. UW CSE 00-02-02, University of Washington, Department of Computer Science and Engineering, Seattle, WA 1

[21] Ni, L. M., Liu, Y., Yiu, C. L., & Patil, A. P. (2003). LANDMARC: Indoor location sensing using active RFID. Proceedings of the First IEEE International Conference on Pervasive Computing and Communications (PerCom 2003), 407-15.

[22] Pradhan, A., Ergen, E., & Akinci, B. (2009). Technological assessment of radio frequency identification technology for indoor localization. Journal of Computing in Civil Engineering, 23(4), 230-8. doi:10.1061/(ASCE)0887-3801(2009)23:4(230)

[23] Liu, H., Darabi, H., Banerjee, P., & Liu, J. (2007). Survey of wireless indoor positioning techniques and systems. IEEE Transactions on Systems, Man, and Cybernetics-Part C (Applications and Reviews), 37(6), 1067-80. doi:10.1109/TSMCC.2007.905750

[24] Sim, R., & Dudek, G. (2003). Comparing image-based localization methods. 18th International Joint Conference on Artificial Intelligence, IJCAI 2003, August 9, 2003 - August 15, 1560-1562.

[25] Randell, C., Djiallis, C., & Muller, H. (2003). Personal position measurement using dead reckoning. 7th IEEE International Symposium on Wearable Computers, ISWC 2003, October 21, 2003 - October 23, 166-175.

[26] Gelb, Arthur. (1974). Applied optimal estimation. MIT press,

[27] Glanzer, G., Bernoulli, T., Wiessflecker, T., & Walder, U. (2009). Semi-autonomous indoor positioning using MEMS-based inertial measurement units and building information. 2009 6th Workshop on Positioning, Navigation and Communication (WPNC'09), 135-9. doi:10.1109/WPNC.2009.4907816

[28] Joshua, L., & Varghese, K. (2011). Accelerometer-based activity recognition in construction. Journal of Computing in Civil Engineering, 25(5), 370-9. doi:10.1061/(ASCE)CP.1943-5487.0000097

[29] Taneja, S., Akcamete, A., Akinci, B., Garrett, J. H., J., Soibelman, L., & East, E. W. (2012). Analysis of three indoor localization technologies for supporting operations and maintenance field tasks. Journal of Computing in Civil Engineering, 26(6), 708-19. doi:10.1061/(ASCE)CP.1943-5487.0000177

[30] Schot, S. H. (1978). Jerk: The time rate of change of acceleration. American Journal of Physics, 46(11), 1090-4. doi:10.1119/1.11504

[31] Aoki, T., Shimogaki, Y., Ikki, T., Tanikawara, M., Sugimoto, S., Kubo, Y., & Fujimoto, K. (2009). Cycle slip detection in kinematic GPS with a jerk model for land vehicles. International Journal of Innovative Computing, Information & Control, 5(1), 153-66.

[32] Liu, C., Gazis, D. C., & Kennedy, T. W. (1999). Human judgment and analytical derivation of ride quality. Transportation Science, 33(3), 290-7. doi:10.1287/trsc.33.3.290

[33] Hrovat, D., & Hubbard, M. (1987). A comparison between jerk optimal and acceleration optimal vibration isolation. Journal of Sound and Vibration, 112(2), 201-10. doi:10.1016/S0022-460X(87)80189-X

[34] R.W. Clough and J. Penzien, Dynamics of Structures, McGraw- Hill, NewYork, NY,USA,

1993.

[35] A. K. Chopra, Dynamics of Structures: Theory and Applications to Earthquake Engineering, Prentice-Hall, New Delhi, India, 2007.

[36] Kalman, Rudolph Emil. (1960). A new approach to linear filtering and prediction problems. Journal of Fluids Engineering 82.1: 35-45.

[37] Anderson, Brian DO, and John B. Moore. (2012). Optimal filtering. Courier Corporation